

# Sensitivity of the $K\beta''$ X-ray Emission Line to Coordination Changes in $\text{GeO}_2$ and $\text{TiO}_2$

G. Spiekermann,\* Ch. J. Sahle,\* J. Niskanen, K. Gilmore, S. Petitgirard, C. Sternemann, J. S. Tse, and M. Murakami



Cite This: *J. Phys. Chem. Lett.* 2023, 14, 1848–1853



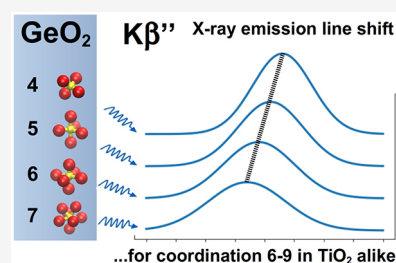
Read Online

ACCESS |

Metrics & More

Article Recommendations

**ABSTRACT:** The hard X-ray  $K\beta''$  emission line shows sensitivity with respect to a wide range of cation–ligand coordination, which we investigate in the cases of  $\text{GeO}_2$  and  $\text{TiO}_2$  on the basis of ab initio spectral calculations on amorphous and crystalline structures. In compressed amorphous  $\text{GeO}_2$ , the sampling of a large number of instantaneous coordination polyhedra from an ab initio molecular dynamics trajectory reveals that the functional relation between the  $K\beta''$  shift and coordination is close to linear between 4-fold and 7-fold coordination. A similar sensitivity of the  $K\beta''$  emission line exists in the coordination range between six and nine of crystalline high-pressure  $\text{TiO}_2$  polymorphs. Our results demonstrate the potential of the  $K\beta''$  emission line in research on the structure of amorphous oxide material.



Coordination changes are of interest in high-pressure research, where the average cation coordination in various amorphous compounds like  $\text{GeO}_2$ ,  $\text{TiO}_2$ , and  $\text{SiO}_2$  at extreme pressures has received considerable attention in the past years but is challenging to access experimentally.<sup>1–6</sup> In these systems, the cations undergo an increase of average coordination number (CN) with pressure, from four to six or above in the case of germanium and silicon and from six to nine or above in the case of titanium oxide.<sup>1–3,6,7</sup> However, there are contradicting results between different studies concerning the onset of average coordination above six in the case of silicon oxide and its analogue germanium oxide.<sup>2–5</sup> This situation calls for validation of novel approaches, for which we study the potential of the  $K\beta''$  X-ray emission line as a probe. The cation  $K\beta''$  X-ray emission line is one of the weakest features in valence-to-core X-ray emission spectroscopy (vtc XES) of chemical systems with cation–ligand (or metal–ligand) bonds.<sup>8</sup> It reflects the valence orbital hybridization with the 2s orbitals of the coordinating ligands, as evidenced in projected electronic density-of-states (pDOS) calculations.<sup>5,9–11</sup> The  $K\beta''$  line is also termed “crossover” transition and is absent in any vtc XES spectrum of a cation in its elemental form. It is known to allow for insight into several aspects of the first ligand coordination shell around the probed atom, such as chemical sensitivity, cation–ligand bond length, and—the target of this study—CN.<sup>8,9,11–25</sup>

The chemical sensitivity of the  $K\beta''$  line with respect to the type of ligand results from differences in binding energy of the *ns* electrons of the ligands, e.g., about 5 eV between nitrogen and oxygen, and has been demonstrated in a variety of studies on e.g. Ti, V, Mn, Fe, Cr, Cu, and Nb.<sup>8,9,11–25</sup> The sensitivity of the  $K\beta''$  line with respect to cation–ligand bond length has

been demonstrated in e.g. Mn, V, Ti, and Ge systems<sup>5,12–14,23</sup> and results from the variable extent of overlap between the ligands’ *ns* orbitals with the valence orbitals of the cation: When the bond length shortens, the overlap increases, leading to a higher “crossover” transition probability and therefore to a more intense  $K\beta''$  line.<sup>8</sup> Its sensitivity with respect to coordination has been discussed for a narrow range of coordination states for nickel, iron, and copper,<sup>11,26,27</sup> but investigations of a wider coordination range are scarce.<sup>5</sup>

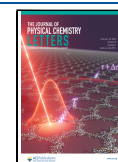
In this work we validate  $K\beta''$  spectroscopy as a probe for an extended range of coordination states: First, we quantitatively assess the functional relation between the  $K\beta''$  line shift and coordination in the case of compressed amorphous  $\text{GeO}_2$ . Second, we qualitatively investigate the applicability of the  $K\beta''$  line shift to different crystalline high-pressure polymorphs of  $\text{TiO}_2$ . Our methods are the ab initio computation of vtc XES spectra of cations in known coordination states using the OCEAN code<sup>28,29</sup> and their evaluation in terms of the  $K\beta''$  line shift.

$\text{GeO}_2$  is well-suited to quantitatively investigate the  $K\beta''$  emission line shift over a wide range of coordination, for two reasons: First, the  $K\beta$  vtc XES spectra of germanium oxide show a free-standing  $K\beta''$  line, well separated from the neighboring  $K\beta_5$  and  $K\beta_2$  emission lines. Second, gradually

Received: January 3, 2023

Accepted: February 7, 2023

Published: February 13, 2023



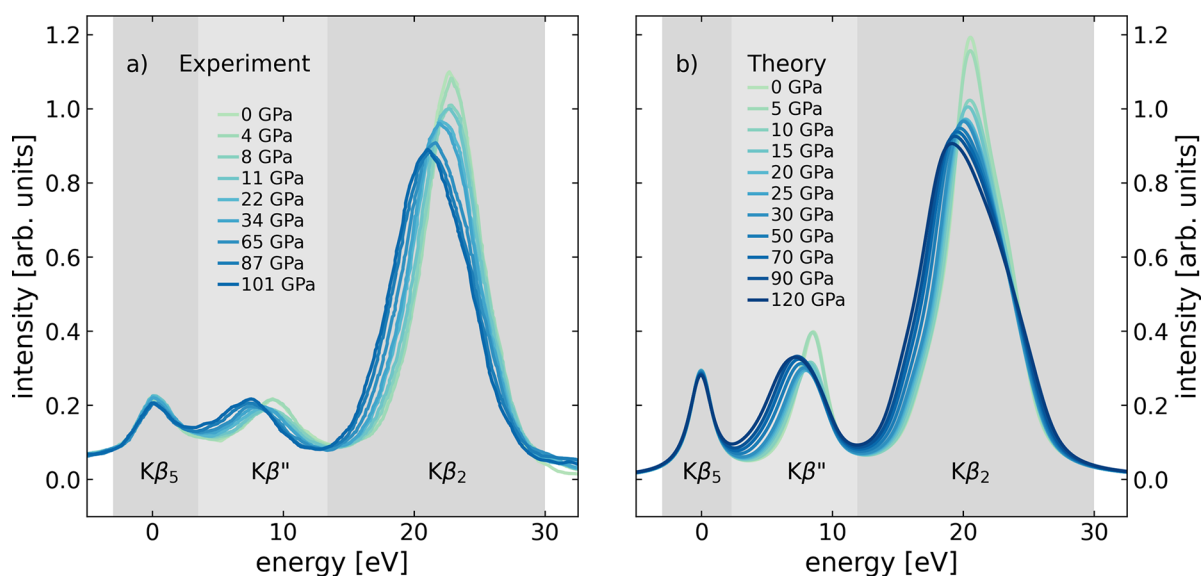


**Figure 1.** (a) Experimental  $K\beta$  valence-to-core X-ray emission spectra of compressed amorphous  $\text{GeO}_2$  from inside a diamond anvil cell at pressures between ambient and 101 GPa.<sup>5</sup> (b) Calculated spectra of compressed amorphous  $\text{GeO}_2$ . At each pressure step of the ab initio molecular dynamics simulation, averaged spectra over all individual Ge sites are shown, aligned to a common position of the  $K\beta_5$  emission line.

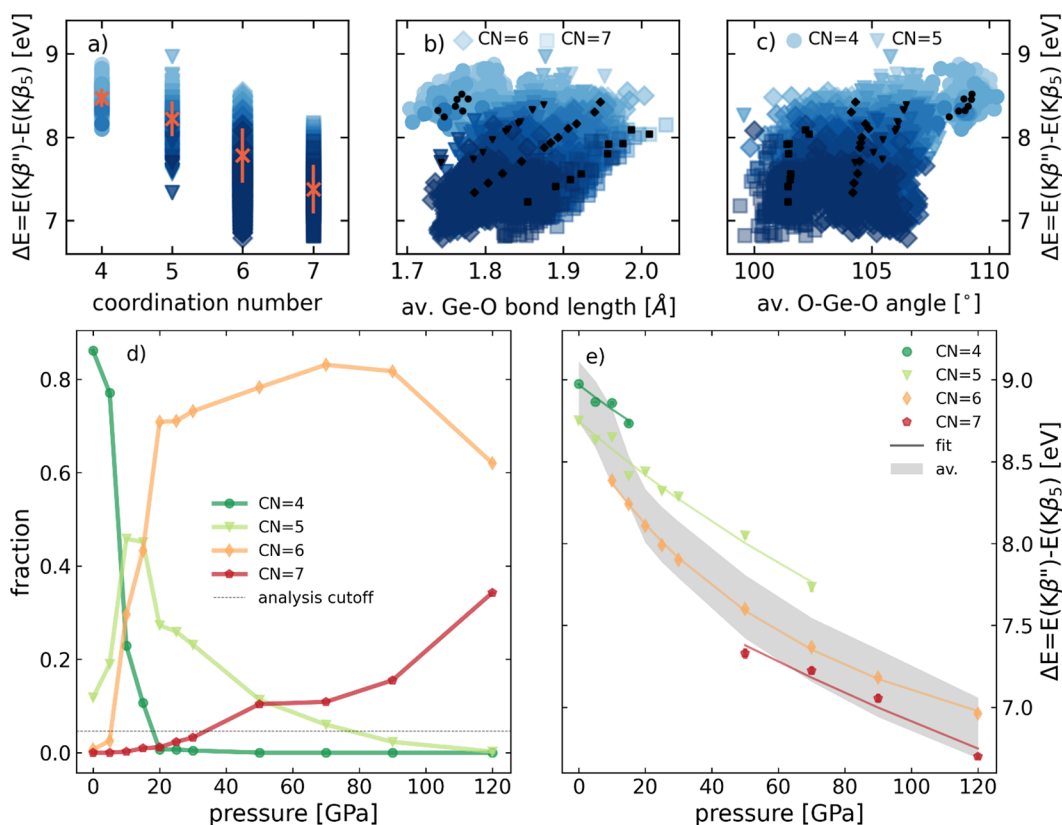


**Figure 2.** (a–c) Energy difference  $\Delta E$  of the Ge  $K\beta''$  emission line relative to the constant  $K\beta_5$  line as a function of coordination (a), the average Ge–O bond length (b), and the mean O–Ge–O angle (c). Crosses in (a) denote the average values, and black symbols in (b) and (c) denote coordination-specific averages. (d) Ge–O coordination number analysis of the MD simulation reported by Du et al.<sup>1</sup> with a radial cutoff of 2.3 Å. (e) Position of the coordination-specific  $K\beta''$  emission line shifting with pressure, expressed as  $\Delta E$  relative to the constant position of the  $K\beta_5$  line, each trend with an exponential fit (solid lines).

compressed amorphous  $\text{GeO}_2$  covers coordination states between 4-fold at ambient pressure and 6-fold at about 20 GPa. Furthermore, the  $K\beta_5$  line serves as inherent calibration reference because its emission energy is not affected by any structural change: The filled and contracted semicore 3d

orbitals in germanium oxide follow the trend of the germanium 1s energy level so closely that the resulting emission energy remains constant within experimental uncertainty (see experimental data in Figure 1a, taken from ref 5). Thus, if considered relative to the energy of the  $K\beta_5$  line

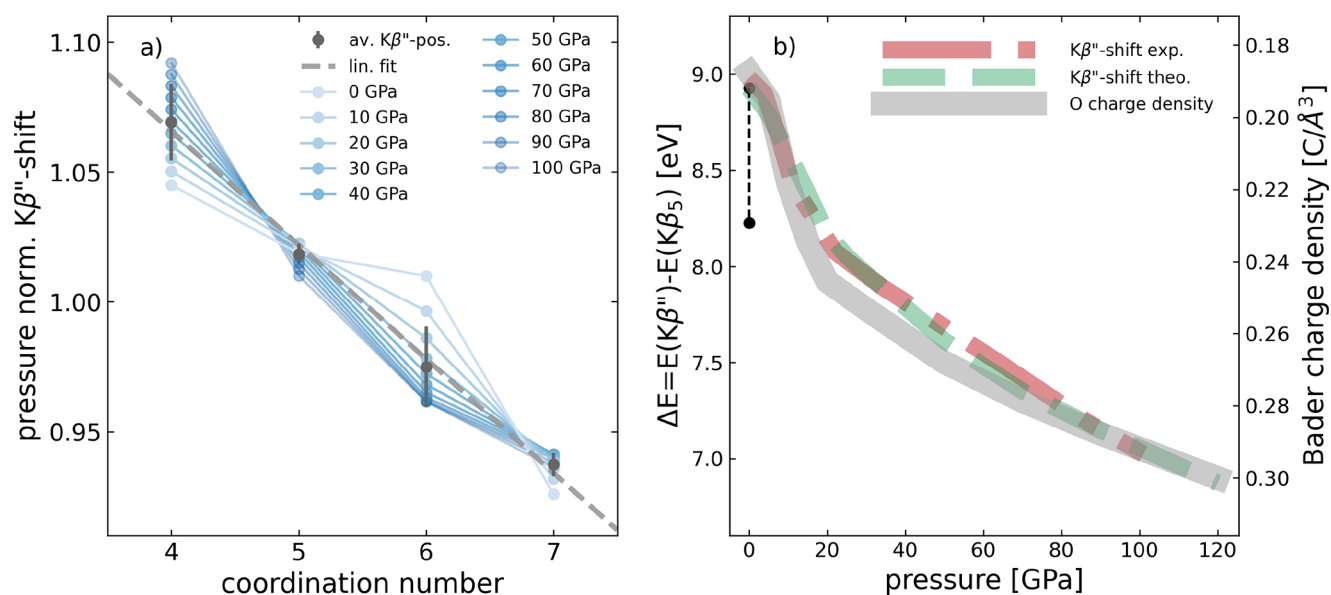


**Figure 3.** (a) Normalized shift of the  $K\beta''$  emission line as a function of coordination, at each pressure step separately (see text for details). Data points are taken from the fits shown in Figure 2e, partially extrapolated to higher or lower pressure. On average, the correlation follows a linear trend (dashed line). (b) Comparison between the shift of the  $K\beta''$  line and the Bader charge density at the oxygen sites (left and right y-axis, respectively) as a function of pressure. The black dumbbell marks the measured difference of 0.7 eV of the  $K\beta''$  emission line position between  $\text{GeO}_2$  with 4- and 6-fold coordination at ambient pressure.<sup>5</sup>

shift can be evaluated from spectra without the need of a precise XES energy calibration.<sup>5</sup>

We performed spectral calculations from a large number of configurations of a previously reported *ab initio* molecular dynamics (AIMD) simulation of amorphous  $\text{GeO}_2$  up to 120 GPa.<sup>1,30</sup> In this way, the ensemble of constant composition allows to sample a large number and variety of independent coordination polyhedra over a wide range of pressures, covering an extended structural parameter space, e.g., with virtually continuously varying degrees of distortion.<sup>31</sup> This broad sampling of the phase space of the coordination shell in the case of amorphous  $\text{GeO}_2$  allows for a quantitative evaluation, establishing a functional dependence between  $K\beta''$  line shift and the cation CN.

Such extended sampling of the coordination shell parameters in amorphous  $\text{GeO}_2$  leads to high agreement between computed and experimental spectra: We summed at each pressure between 0 and 120 GPa 360 individual vtc XES spectra (72 Ge atoms in five uncorrelated AIMD configurations) and compare the sum (Figure 1b) to experimental spectra (Figure 1a). Experimental spectra were taken from ref 5. In addition, we also show the measured  $K\beta_2$  line to better illustrate the quality of the agreement between theory and experiment. The overall line shape and the pressure-induced relative changes of the entire experimental spectrum are well reproduced by the simulated spectra, which lends credibility to the spectral calculations.

Our focus on coordination number, rather than on mean cation–ligand bond length or mean polyhedral bond angle, deserves a brief explanation. In fact, each spectrum may hold information about a variety of parameters of the first coordination shell.<sup>31</sup> We evaluated all individual Ge spectra, irrespective of pressure, in terms of the  $K\beta''$  line shift (here and in the following expressed as  $\Delta E$ , i.e., the difference in emission energy of the  $K\beta''$  line relative to the constant  $K\beta_5$  line) and plot  $\Delta E$  against CN, mean cation–ligand bond length, and mean polyhedral bond angle in Figure 2a–c. All three

parameters are computed for the oxygen atoms found within the first coordination shells, defined by a sphere of 2.3 Å radius centered around the active Ge site.<sup>1</sup> The correlation between the  $K\beta''$  emission line shift and CN is evident and on average even close to linear (Figure 2a). From the trends as a function of bond length and angle, it is visible that there are clear correlations when the coordination is taken into account (see black symbols for coordination-specific averages in Figure 2b). However, these coordination-specific trends can be applied to experimental results only after coordination is known. For this reason, we focus here on the dependency of the  $K\beta''$  line shift on coordination. Beyond the scope of this work is the correlation of the  $K\beta''$  emission line intensity with bond distance, established in a number of works.<sup>5,12–14,23</sup>

The distribution of coordination states in the simulation is shown in Figure 2d as a function of pressure: 4-fold Ge–O coordination is dominant at pressures up to 20 GPa and 6-fold is dominant at higher pressure, with a fraction of 5-fold present throughout and 7-fold appearing at 50 GPa.<sup>1</sup> For the correlation between the  $K\beta''$  line shift and CN, at each pressure, we consider only those coordination states that have a relative abundance of at least 5% to ensure a meaningful sampling (dashed horizontal line in Figure 2d), leading to four different coordination states between four and seven.

Next, we investigated the relation between the  $K\beta''$  emission line shift and CN over the entire pressure range. For this, we first averaged a large number of individual spectra of identical CN at each pressure step of the simulation. The resulting coordination-specific dependency of  $\Delta E$  on pressure reveals four trends of similar slope, offset from each other by a few 100 meV (Figure 2e, exponential decay fits indicated by lines). These offsets between the coordination-specific trends of  $\Delta E$  are evidence for the sensitivity of the  $K\beta''$  line with respect to coordination. With information about the pressure-dependent magnitude of these offsets between each coordination-specific pressure trend, the average coordination number in amorphous  $\text{GeO}_2$  can be determined from two parameters: the pressure of

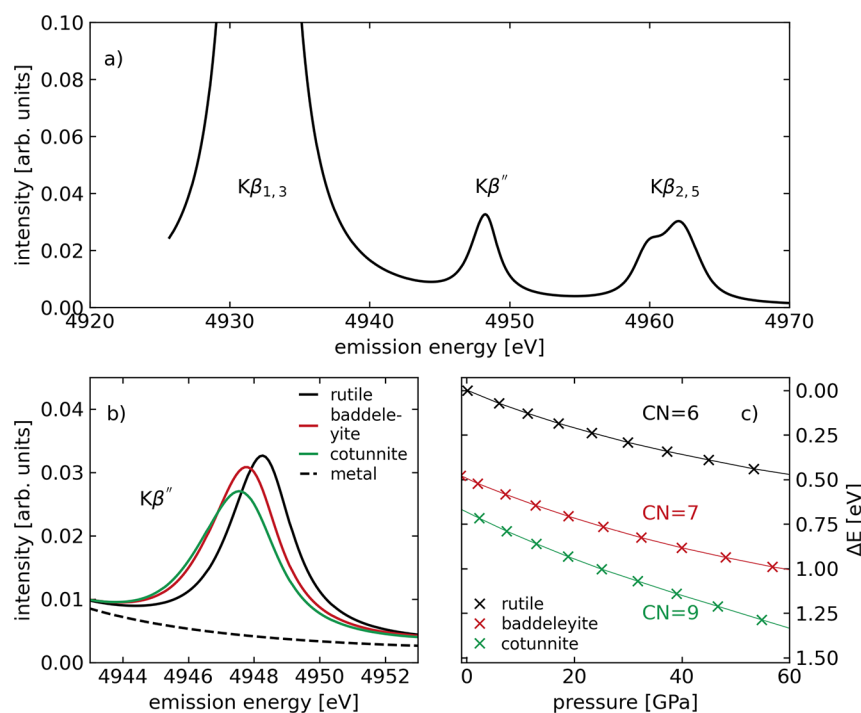


**Figure 4.** (a) Computed vtc XES spectrum of rutile-TiO<sub>2</sub>. (b) Zoom into the Ti Kβ'' emission line of calculated vtc XES spectra of TiO<sub>2</sub> polymorphs: rutile, baddeleyite, and cotunnite structure of 6-, 7-, and 9-fold coordination, respectively, all near ambient pressure. The spectrum of metallic titanium is shown for reference (dashed line). (c) shift of the titanium Kβ'' emission line of these polymorphs as a function of pressure, as obtained in the computed spectra, expressed as ΔE relative to the Kβ'' line position of rutile-structured TiO<sub>2</sub> at ambient pressure.

the system and the position of the Kβ'' line, which can be determined in experimental spectra with an uncertainty of <100 meV. For illustration, the computed total trend with pressure of ΔE of all germanium atoms (shown as a gray trend in Figure 2e, its width of about 0.4 eV representing the scatter of all computed spectra at a given pressure) is the experimentally accessible quantity, from which the average coordination can be inferred, when the coordination-specific trends are known.<sup>5</sup>

As the coordination-specific trends in the case of amorphous GeO<sub>2</sub> have slightly different slopes (Figure 2e), the offsets between the coordination-specific trends of ΔE vary with pressure. We elucidate this pressure dependence by calculating ΔE as a function of coordination for ten pressure points between 0 and 100 GPa separately (Figure 3a), yielding curves equivalent to vertical cuts through the fits shown in Figure 2e and their extrapolation. Normalized to the mean Kβ'' shift and averaged over all pressures, the data show a close-to-linear shift of the Kβ'' line with coordination (dashed line in Figure 3a).

The origin of the Kβ'' line shift, although not the main focus of this study, deserves some attention. The previously computationally observed increased oxygen charge density in compressed amorphous GeO<sub>2</sub> and SiO<sub>2</sub> has been interpreted as increasing ionic character of these compounds.<sup>1</sup> Also on the basis of charge density, an increase in ionicity had been stated before for the transition from 4-fold to 6-fold coordination in crystalline GeO<sub>2</sub> and SiO<sub>2</sub> compounds of quartz- and rutile-like structure at ambient pressure.<sup>32,33</sup>

To align with these previous observations, we computed the oxygen Bader charge density and show its average at each pressure as gray curve in Figure 3b (right y-axis). It is found to increase monotonically with pressure, with a strong increase of charge density at the oxygen site by about 30% in the pressure

range from 0 to about 20 GPa, in which the coordination increases from 4-fold to predominantly 6-fold. Because of the general volume compression, also the charge density at the Ge sites increases (not shown), but considerably less in both absolute and relative values. Interestingly, the evolution with pressure of the shift of the Kβ'' line to lower emission energy correlates with the increase of charge density at the oxygen site over the entire pressure range (Figure 3, left y-axis). Furthermore, the measured Kβ'' line shift at ambient pressure of 0.7 eV between the quartz-like structure and the rutile-like structure (shown as black dumbbell mark in Figure 3b) anticipates the coordination-change induced high-pressure trend up to about 20 GPa.

X-ray emission spectroscopy, rather than recording absolute shifts, records the difference between the 1s core level and valence levels. When both levels shift the same amount of energy, e.g., due to change in Madelung potential, there is no observable shift. This is the case for the contracted Ge 3d states, whose transition line Kβ<sub>5</sub> remains constant in emission energy across all recorded spectra. The Kβ'' shift of 0.7 eV at ambient pressure, due to increased coordination at the simultaneous 8% increase of bond length, shows that coordination is the strongest single factor influencing the Kβ'' shift. A difference in relative population of germanium 4s and 4p orbitals, both hybridized with oxygen 2s, is thus probably the strongest factor causing the observed Kβ'' shift, followed by bond shortening. The accompanying contraction of the volume leads to the correlation of the oxygen charge density and the Kβ'' line shift as shown in Figure 3b.

The second aim of our study is to demonstrate qualitatively the potential of our approach to study other cations and higher CN range. This is illustrated on TiO<sub>2</sub>. TiO<sub>2</sub> is a good choice for two reasons: First, the Kβ'' emission line is free-standing in

the vtc XES spectrum of titanium compounds, in calculation and experiment separated from the neighboring  $K\beta_{1,3}$  and  $K\beta_{2,5}$  lines (Figure 4a).<sup>13,14,17,20–23,25</sup> Second, the crystalline high-pressure polymorphs of  $TiO_2$  cover an unusual and wide range of coordination states: The crystalline high-pressure  $TiO_2$  polymorphs are rutile-type,  $ZrO_2$ -type (baddeleyite), and  $PbCl_2$ -type (cotunnite) structures, with 6-, 7-, and 9-fold coordination of titanium, respectively.<sup>34,35</sup> A crystalline structure of titanium in 8-fold coordination has not been found experimentally, to the best of our knowledge.

Our calculated vtc XES spectrum of rutile- $TiO_2$  is in reasonable agreement with experimental data (see, e.g., refs 23 and 25) and shows the  $K\beta_{1,3}$ ,  $K\beta''$ , and  $K\beta_{2,5}$  lines separated from each other (Figure 4a). The simulated spectra of the three  $TiO_2$  polymorphs of the rutile-,  $ZrO_2$ -, and  $PbCl_2$ -type with 6-, 7-, and 9-fold coordination (and of metallic titanium as reference) are shown in Figure 4b, normalized to the area of the  $K\beta_{1,3}$  line. The  $K\beta''$  line shifts from one polymorph to the other by a few 100 meV at ambient pressure, while being absent in the case of metallic Ti, as expected.

Next, we compressed the unit cells of the three polymorphs in steps and computed the vtc XES spectrum and the pressure at each pressure. This allowed us to assess the coordination-specific  $K\beta''$  line shift as a function of pressure (Figure 4c). Here we consider its shift as relative to the position in rutile- $TiO_2$  at ambient pressure, in lack of an inherent calibrating emission line as the  $K\beta_5$  line in the case of  $GeO_2$ .<sup>36</sup>

The  $K\beta''$  line shift between the different  $TiO_2$  polymorphs at ambient pressure is persistent at high pressure and amounts to about 0.5 eV between 6- and 7-fold coordinated titanium and to 0.3 eV between 7- and 9-fold coordinated titanium. The functional relation between coordination and the  $K\beta''$  line shift thus is not linear in this case of strictly crystalline structures of  $TiO_2$ . The spectra of crystalline structures lack a sampling of the parameter space of the first coordination shell and may therefore be biased.<sup>37</sup> However, the trends in Figure 4 are encouraging to further investigate this dependency in the case of amorphous titanium compounds.<sup>6</sup>

There is a number of elements to which the  $K\beta''$  emission line evaluation can be applied as done here. We hypothesize that the approach is not limited to the oxides of a single cation: With appropriate reference samples and computational support, oxides with several cations could be investigated, allowing for special insight, as diffraction-based techniques can reach their limit when investigating coordination in multi-component oxides. This approach can provide a unique means of structural investigation of chemically complex, amorphous material at high pressure or in other confined sample environments.

In summary, we have elucidated quantitatively the sensitivity of the  $K\beta''$  emission line with respect to an extended range of coordination states in the case of compressed amorphous  $GeO_2$ . Pressure as a canonical variable and the extensive sampling of the structural parameters in the AIMD simulation of amorphous  $GeO_2$  allowed us to quantify the shift observed in the  $K\beta''$  line of Ge as a function of coordination state beyond structural bias. The functional relation between the position of the  $K\beta''$  line and the cation–ligand coordination between four and seven was found to be nearly linear. The origin of the shift lies primarily in a relative change in the hybridization between oxygen 2s and metal cation valence orbitals, and to a lesser extent in the amount of overlap, increased by shortening of bonds. Computed spectra of high-

pressure  $TiO_2$  polymorphs reveal a consistent sensitivity with respect to even higher coordination in the range between six and nine. This approach can provide new insight into the debated coordination evolution in compressed amorphous oxides. The application to chemically more complex oxides seems possible but needs additional investigation.

## AUTHOR INFORMATION

### Corresponding Authors

G. Spiekermann – ETH Zürich, 8092 Zürich, Switzerland;

orcid.org/0000-0002-3732-6915; Email: gspiekerm@ethz.ch

Ch. J. Sahle – European Synchrotron Radiation Facility (ESRF), 38000 Grenoble, France; orcid.org/0000-0001-8645-3163; Email: christoph.sahle@esrf.fr

### Authors

J. Niskanen – Department of Physics and Astronomy, University of Turku, 20014 Turun yliopisto, Finland

K. Gilmore – Physics Department and IRIS Adlershof, Humboldt Universität zu Berlin, 12489 Berlin, Germany

S. Petitgirard – ETH Zürich, 8092 Zürich, Switzerland

C. Sternemann – Technische Universität Dortmund, Fakultät Physik/DELTA, 44227 Dortmund, Germany; orcid.org/0000-0001-9415-1106

J. S. Tse – Department of Physics and Engineering Physics, University of Saskatchewan, Saskatoon S7N 5E2, Canada; orcid.org/0000-0001-8389-7615

M. Murakami – ETH Zürich, 8092 Zürich, Switzerland

Complete contact information is available at:

<https://pubs.acs.org/10.1021/acs.jpcllett.3c00017>

### Notes

The authors declare no competing financial interest.

## ACKNOWLEDGMENTS

G.S. is grateful to Wayne Nesbitt for an insightful discussion. J.N. thanks the Academy of Finland for Project 331234. J.S.T. acknowledges NSERC Canada for a Discovery Grant. M.M. acknowledges ETH Zürich for support from the ETH Start-Up Fund. The ESRF is acknowledged for providing computing resources.

## REFERENCES

- (1) Du, X.; Tse, J. S. Oxygen packing fraction and the structure of silicon and germanium oxide glasses. *J. Phys. Chem. B* **2017**, *121*, 10726–10732.
- (2) Prescher, C.; Prakapenka, V. B.; Stefanski, J.; Jahn, S.; Skinner, L. B.; Wang, Y. Beyond sixfold coordinated Si in  $SiO_2$  glass at ultrahigh pressures. *Proc. Natl. Acad. Sci. U. S. A.* **2017**, *114*, 10041.
- (3) Petitgirard, S.; Sahle, C.J.; Weis, C.; Gilmore, K.; Spiekermann, G.; Tse, J.S.; Wilke, M.; Cavallari, C.; Cerantola, V.; Sternemann, C. Magma properties at Earth's lower mantle conditions inferred from electronic structure and coordination of silica. *Geochem. Perspect. Lett.* **2019**, *9*, 32–37.
- (4) Kono, Y.; Kenney-Benson, C.; Ikuta, D.; Shibasaki, Y.; Wang, Y.; Shen, G. Ultrahigh-pressure polyamorphism in  $GeO_2$  glass with coordination number > 6. *Proc. Natl. Acad. Sci. U. S. A.* **2016**, *113*, 3436–3441.
- (5) Spiekermann, G.; Harder, M.; Gilmore, K.; Zalden, P.; Sahle, C. J.; Petitgirard, S.; Wilke, M.; Biedermann, N.; Weis, C.; Morgenroth, W.; et al. Persistent octahedral coordination in amorphous  $GeO_2$  up to 100 GPa by  $K\beta''$  x-ray emission spectroscopy. *Phys. Rev. X* **2019**, *9*, 011025.

- (6) Shu, Y.; Kono, Y.; Ohira, I.; Li, Q.; Hrubciak, R.; Park, C.; Kenney-Benson, C.; Wang, Y.; Shen, G. Observation of 9-fold coordinated amorphous  $\text{TiO}_2$  at high pressure. *J. Phys. Chem. Lett.* **2020**, *11*, 374–379.
- (7) Kim, Y.-H.; Yi, Y. S.; Kim, H.-I.; Chow, P.; Xiao, Y.; Shen, G.; Lee, S. K. Pressure-driven changes in the electronic bonding environment of  $\text{GeO}_2$  glass above megabar pressures. *J. Am. Chem. Soc.* **2022**, *144*, 10025–10033.
- (8) Glatzel, P.; Bergmann, U. High resolution 1s core hole x-ray spectroscopy in 3d transition metal complexes - electronic and structural information. *Coord. Chem. Rev.* **2005**, *249*, 65–95.
- (9) Ravel, B.; Kropf, A.; Yang, D.; Wang, M.; Topsakal, M.; Lu, D.; Stennett, M.; Hyatt, N. Nonresonant valence-to-core x-ray emission spectroscopy of niobium. *Phys. Rev. B* **2018**, *97*, 125139.
- (10) March, A.; Assefa, T.; Boemer, C.; Bressler, C.; Britz, A.; Diez, M.; Doumy, G.; Galler, A.; Harder, M.; Khakhulin, D.; et al. Probing transient valence orbital changes with picosecond valence-to-core x-ray emission spectroscopy. *J. Phys. Chem. C* **2017**, *121*, 2620–2626.
- (11) Zhang, R.; Li, H.; McEwen, J. Chemical sensitivity of valence-to-core X-ray emission spectroscopy due to the ligand and the oxidation state: A computational study on Cu-SSZ-13 with multiple  $\text{H}_2\text{O}$  and  $\text{NH}_3$  adsorption. *J. Phys. Chem. C* **2017**, *121*, 25759.
- (12) Bergmann, U.; Horne, C.; Collins, T.; Workman, J.; Cramer, S. Chemical dependence of interatomic X-ray transition energies and intensities – a study of Mn  $K\beta''$  and  $K\beta_{2,5}$  spectra. *Chem. Phys. Lett.* **1999**, *302*, 119–124.
- (13) Fazinic, S.; Jaksic, M.; Mandic, L.; Dobrinic, J. Chemical dependence of second-order radiative contributions in the  $K\beta$  x-ray spectra of vanadium and its compounds. *Phys. Rev. A* **2006**, *74*, 062501.
- (14) Mandic, L.; Fazinic, S.; Jaksic, M. Chemical effects on the  $K\beta''$  and  $K\beta_{2,5}$  X-ray lines of titanium and its compounds. *Phys. Rev. A* **2009**, *80*, 042519.
- (15) Safonova, O. V.; Florea, M.; Bilde, J.; Delichere, P.; Millet, J. M. M. Local environment of vanadium in V/Al/O-mixed oxide catalyst for propane ammoxidation: characterization by in situ valence-to-core x-ray emission spectroscopy and X-ray absorption spectroscopy. *J. Catal.* **2009**, *268*, 156–164.
- (16) Eeckhout, S.; Safonova, O.; Smolentsev, G.; Biasioli, M.; Safonov, V.; Vykhodtseva, L.; Sikora, M.; Glatzel, P. Cr local environment by valence-to-core X-ray emission spectroscopy. *J. Anal. At. Spectrom.* **2009**, *24*, 215–223.
- (17) Swarbrick, J. C.; Kvashnin, Y.; Schulte, K.; Seenivasan, K.; Lamberti, C.; Glatzel, P. Ligand identification in titanium complexes using x-ray valence-to-core emission spectroscopy. *Inorg. Chem.* **2010**, *49*, 8323–8332.
- (18) Delgado-Jaime, M.; Dible, B.; Chiang, K.; Brennessel, W.; Bergmann, U.; Holland, P.; DeBeer, S. Identification of a single light atom within a multinuclear metal cluster using valence-to-core x-ray emission spectroscopy. *Inorg. Chem.* **2011**, *50*, 10709–10717.
- (19) Pollock, C. J.; DeBeer, S. Valence-to-core x-ray emission spectroscopy: a sensitive probe of the nature of a bound ligand. *J. Am. Chem. Soc.* **2011**, *133*, 5594–5601.
- (20) Seenivasan, K.; Gallo, E.; Piovano, A.; Vitillo, J. G.; Sommazzi, A.; Bordiga, S.; Lamberti, C.; Glatzel, P.; Groppo, E. Silica-supported Ti chloride tetrahydrofuranates, precursors of Ziegler–Natta catalysts. *Dalton Trans* **2013**, *42*, 12706.
- (21) Gallo, E.; Bonino, F.; Swarbrick, J. C.; Petrenko, T.; Piovano, A.; Bordiga, S.; Gianolio, D.; Groppo, E.; Neese, F.; Lamberti, C.; et al. Preference towards five-coordination in Ti silicalite-1 upon molecular adsorption. *ChemPhysChem* **2013**, *14*, 79–83.
- (22) Gallo, E.; Piovano, A.; Marini, C.; Mathon, O.; Pascarelli, S.; Glatzel, P.; Lamberti, C.; Berlier, G. Architecture of the Ti(IV) sites in TiAlPO-5 determined using Ti K-edge x-ray absorption and x-ray emission spectroscopies. *J. Phys. Chem. C* **2014**, *118*, 11745–11751.
- (23) Wansleben, M.; Vinson, J.; Holfelder, I.; Kayser, Y.; Beckhoff, B. Valence-to-core X-ray emission spectroscopy of Ti,  $\text{TiO}$ , and  $\text{TiO}_2$  by means of a double full-cylinder crystal von Hamos spectrometer. *Xray Spectrom* **2019**, *48*, 102–106.
- (24) Jahrman, E. P.; Holden, W. M.; Govind, N.; Kas, J. J.; Rana, J.; Piper, L. F. J.; Siu, C.; Whittingham, M. S.; Fister, T. T.; Seidler, G. T. Valence-to-core x-ray emission spectroscopy of vanadium oxide and lithiated vanadyl phosphate materials. *J. Mater. Chem. A* **2020**, *8*, 16332.
- (25) Miaja-Avila, L.; O'Neil, G. C.; Joe, Y. I.; Morgan, K. M.; Fowler, J. W.; Doriese, W. B.; Ganly, B.; Lu, D.; Ravel, B.; Swetz, D. S.; et al. Valence-to-core x-ray emission spectroscopy of titanium compounds using energy dispersive detectors. *Xray Spectrom* **2021**, *50*, 9–20.
- (26) Phu, P.; Gutierrez, C.; Kundu, S.; Sokaras, D.; Kroll, T.; Warren, T.; Stieber, S. Quantification of Ni-N-O bond angles and NO activation by x-ray emission spectroscopy. *Inorg. Chem.* **2021**, *60*, 736–744.
- (27) Stieber, S.; Milsman, C.; Hoyt, J.; Turner, Z.; Finkelstein, K.; Wiegardt, K.; DeBeer, S.; Chirik, P. Bis(imino)pyridine iron dinitrogen compounds revisited: differences in electronic structure between four- and five-coordinate derivatives. *Inorg. Chem.* **2012**, *51*, 3770–3785.
- (28) Vinson, J.; Rehr, J.; Kas, J.; Shirley, E. Bethe-Salpeter equation calculation of core excitation spectra. *Phys. Rev. B* **2011**, *83*, 115106.
- (29) Gilmore, K.; Vinson, J.; Shirley, E. L.; Prendergast, D.; Pemmaraju, C. D.; Kas, J. J.; Vila, F. D.; Rehr, J. J. Efficient implementation of core-excitation Bethe–Salpeter equation calculations. *Comput. Phys. Commun.* **2015**, *197*, 109–117.
- (30) The basis for our theoretical investigation of  $\text{GeO}_2$  are atomic structures generated by *ab initio* molecular dynamics (AIMD) simulations of amorphous  $\text{GeO}_2$ , previously reported by Du et al.<sup>1</sup> In short, an amorphous structure was generated by melting a 72  $\text{GeO}_2$  formula units containing supercell of ambient quartz-like solid  $\text{GeO}_2$  at 2800 K within the canonical ensemble (NVT). The melt was subsequently cooled within the isothermal–isobaric ensemble in steps of 300 K. See Du et al.<sup>1</sup> for a full description.
- (31) Niskanen, J.; Sahle, C. J.; Gilmore, K.; Uhlig, F.; Smiatek, J.; Föhlich, A. Disentangling structural information from core-level excitation spectra. *Phys. Rev. E* **2017**, *96*, 013319.
- (32) Gibbs, G. V.; Wallace, A. F.; Cox, D. F.; Downs, R. T.; Ross, N. L.; Rosso, K. M. Bonded interactions in silica polymorphs, silicates, and siloxane molecules. *Am. Mineral.* **2009**, *94*, 1085–1102.
- (33) Nada, R.; Catlow, C. R. A.; Dovesi, R.; Pisani, C. An *ab-initio* Hartree-Fock study of alpha-quartz and stishovite. *Phys. Chem. Miner.* **1990**, *17*, 353–362.
- (34) Dubrovinskaia, N. A.; Dubrovinsky, L. S.; Swamy, V.; Ahuja, R. Cotunnite-structured titanium dioxide. *High Press. Res.* **2002**, *22*, 391–394.
- (35) El Goresy, A.; Chen, M.; Dubrovinsky, L.; Gillet, P.; Graup, G. An ultradense polymorph of rutile with seven-coordinated titanium from the Ries crater. *Science* **2001**, *293*, 1467–1470.
- (36) The  $K\beta_{1,3}$  line is of limited use as reference, as its energy changes by several tens of meV between structures and much more as a function of pressure.
- (37) Lafuerza, S.; Carluantuo, A.; Retegan, M.; Glatzel, P. Chemical sensitivity of  $K\alpha$  and  $K\beta$  x-ray emission from a systematic investigation of iron compounds. *Inorg. Chem.* **2020**, *59*, 12518–12535.